

Clustering of Galaxies with $f(R)$ gravity

Salvatore Capozziello,^{1,2,3,4*} Mir Faizal,^{5,6†} Mir Hameeda,^{7,8‡} Behnam Pourhassan,^{9§}
 Vincenzo Salzano^{10¶} Sudhaker Upadhyay,^{11||}

¹*Dipartimento di Fisica “E. Pancini”, Università di Napoli Federico II, I-80126 - Napoli, Italy*

²*INFN Sez. di Napoli, Compl. Univ. di Monte S. Angelo, Edificio G, I-80126 - Napoli, Italy*

³*Gran Sasso Science Institute (INFN), Viale F. Crispi, 7, I-67100, L’Aquila, Italy*

⁴*Tomsk State Pedagogical University, ul. Kievskaya, 60, 634061 Tomsk, Russia*

⁵*Irving K. Barber School of Arts and Sciences, University of British Columbia - Okanagan, 3333 University Way, Kelowna, British Columbia V1V 1V7, Canada*

⁶*Department of Physics and Astronomy, University of Lethbridge, Lethbridge, Alberta, T1K 3M4, Canada*

⁷*Department of Physics, S.P. Collage, Srinagar, Kashmir, 190001, India*

⁸*Visiting Associate, IUCCA, Pune, 41100, India*

⁹*School of Physics, Damghan University, Damghan, 3671641167, Iran*

¹⁰*Institute of Physics, Faculty of Mathematics and Physics, University of Szczecin, Wielkopolska 15, 70-451 Szczecin, Poland*

¹¹*Centre for Theoretical Studies, Indian Institute of Technology Kharagpur, Kharagpur-721302, India*

Accepted XXX. Received YYY; in original form ZZZ

ABSTRACT

Based on thermodynamics, we discuss the galactic clustering of expanding Universe by assuming the gravitational interaction through the modified Newton’s potential given by $f(R)$ gravity. We compute the corrected N -particle partition function analytically. The corrected partition function leads to more exact equations of states of the system. By assuming that system follows quasi-equilibrium, we derive the exact distribution function which exhibits the $f(R)$ correction. Moreover, we evaluate the critical temperature and discuss the stability of the system. We observe the effects of correction of $f(R)$ gravity on the power law behavior of particle-particle correlation function also. In order to check feasibility of an $f(R)$ gravity approach to the clustering of galaxies, we compare our results with an observational galaxy cluster catalog.

Key words: cosmology: theory – dark energy – large-scale structure of Universe
 — methods: data analysis - analytical

1 OVERVIEW AND MOTIVATIONS

The distribution of galaxies is influenced by the gravitational force (Padilla, et al. 2004). In fact, gravitational force plays an important role not only in clustering of galaxies but also in their large scale structure formation. The characterization of galactic clusters on very large scales is very crucial to understand the evolution and distribution of the galaxies throughout the Universe. One of the standard ways to study the formation of the Universe is study of the correlation functions by means of observation (Peebles 1980) and N -body computer simulations (Itoh et al. 1993). It is known that the gravitating systems, which interact in pairs, the correlation

functions determine the thermodynamical properties which includes gravitation (Hills 1956).

An empirically motivated modification of Newtonian dynamics, so-called MOND, has been proposed at low accelerations (Milgrom 1983), which had explained successfully a number of observational properties of galaxies (Sanders et al. 2002). In MOND scenario, the modified gravitational potential in the weak field limit of $f(R)$ gravity has estimated the total mass of a sample of 12 clusters of galaxies which also fits to the mass of visible matter estimated by X-ray observations (Capozziello et al. 2009). The effects of modified gravitational potential on clustering of galaxies have been studied recently. For instant, the effects of dark energy on galactic clustering is studied in Refs. (Hameeda et al. 2016a; Pourhassan et al. 2017). Recently, the galactic clustering of an expanding Universe by considering the logarithmic and volume (quantum) corrections to Newton’s law along with the repulsive effect of a harmonic force induced by the cosmological constant is also discussed (Upadhyay 2017). The clus-

* E-mail: capozzie@na.infn.it

† E-mail: mirfaizalmir@googlemail.com

‡ E-mail: hme123eda@gmail.com

§ E-mail: b.pourhassan@du.ac.ir

¶ E-mail: vincenzo.salzano@usz.edu.pl

|| E-mail: sudhakerupadhyay@gmail.com

tering of galaxies under brane world modified gravity is also analysed recently (Hameeda et al. 2016b). Our motivation here is to discuss the effects of $f(R)$ gravity on the galactic clustering and compare our results with the observations. For details on these theories see, for example Nojiri & Odintsov. (2011); Capozziello & De Laurentis. (2011, 2012); Nojiri, et al. (2017).

In this paper, we first calculate the modification in the Newtonian potential due to the $f(R)$ gravity. The modified Newtonian potential leads to an explicit form of N -particle (galaxies) configuration integrals which helps us to estimate the N -particle partition function. Once the partition function is known, it is matter of calculation to derive various important thermodynamical entities. For instance, we derive Helmholtz free energy, entropy, internal energy, pressure and chemical potential. Remarkably, the corrected form of clustering parameter emerges naturally from these thermodynamical quantities. With the help of this clustering parameter and generating functional, we derive the exact expression for distribution function for both point and non-point galaxies and study the effects of correction term on the distribution function. Furthermore, we demonstrate the corrected specific heat at constant volume and by maximizing it we compute critical temperature for the gravitating system under $f(R)$ gravity. Remarkably, we obtain the same form of corrected specific heat in terms of critical temperature to that of without correction. Moreover, we analyse the evolution of galaxy-galaxy correlation function where the effects of $f(R)$ modifications are evident. Finally, we have also tried to test the proposed $f(R)$ gravity model by the obtained distribution function with observational data. While we obtain a very good description of the observed clustering of galaxies with our formulas, we have also to stress that we cannot constrain in a statistically significant way most of the $f(R)$ parameters, due to the large degeneracies among them.

The plan of the paper is as following. In section 2, we discuss $f(R)$ gravity and the N particle partition function of the system under the gravitational potential of an analytic $f(R)$ theory. In section 3, we study various thermodynamical equation of states relevant for strongly interacting system of galaxies interacting through the modified Newtonian potential due to $f(R)$ gravity. In section 4, we estimate more exact distribution function for such gravitating system. The critical temperature is derived in section 5. The power law behavior for the galaxy-galaxy correlation function under $f(R)$ modified Newtonian potential is discussed in section 6. The theory is matched with observations in section 7. Finally, we draw conclusions and make final remarks in the last section.

2 GRAVITATIONAL PARTITION FUNCTION

Let us first write the action for $f(R)$ gravity as follows (Capozziello et al. 2009),

$$S = \frac{1}{16\pi G} \int d^4x \sqrt{-g} [f(R) + \mathcal{L}_{matter}], \quad (1)$$

where $f(R)$ is an analytic function of the Ricci scalar R , g refers the determinant of the metric $g_{\mu\nu}$ and \mathcal{L}_{matter} is the standard Lagrangian for the perfect fluid matter. The

equations of motion corresponding to the metric is given by

$$f' R_{\mu\nu} - \frac{1}{2} g_{\mu\nu} f'_{;\mu\nu} + g_{\mu\nu} \square f' = 8\pi G T_{\mu\nu}, \quad (2)$$

where the prime indicates the derivative with respect to R . Here $T_{\mu\nu}$ is the energy momentum tensor of matter given as $T_{\mu\nu} = \frac{-2}{\sqrt{-g}} \frac{\delta(\sqrt{-g} \mathcal{L}_{matter})}{\delta g^{\mu\nu}}$. In order to study the most general result, we only consider analytic Taylor expandable functions

$$f(R) \simeq f_0 + f_1 R + f_2 R^2 + \dots \quad (3)$$

Here f_1 and f_2 are the expansion coefficients and dots include higher order terms (Huang 2014) and also logarithmic corrected term (Sadeghi et al. 2016).

In order to discuss the physical prescription of the asymptotic flatness at infinity, the metric becomes (Capozziello et al. 2009),

$$ds^2 = \left[1 - \frac{2GM}{f_1 r} - \frac{\delta_1(t) e^{-r\sqrt{-\xi}}}{3\xi r} - \frac{\Lambda r^2}{3} \right] dt^2 - \left[1 + \frac{2GM}{f_1 r} - \frac{\delta_1(t)(r\sqrt{-\xi} + 1)e^{-r\sqrt{-\xi}}}{3\xi r} \right] dr^2 - r^2 d\Omega, \quad (4)$$

where the integration constant $\delta_1(t)$ is arbitrary time-function and has the dimensions of $length/time^2$, and $d\Omega$ is the angular element. Here $\xi = \frac{f_1}{6f_2}$ has the dimension of $1/(length)^2$, with f_1 being dimensionless, and f_2 having the dimension of $(length)^2$.

As we have an explicit Newtonian-like term into the definition, the solution can be given in terms of gravitational potential $U(r)$. In particular, it is $g_{tt} = 1 + 2U(r)$ and then from (4) the gravitational potential of an analytic $f(R)$ -theory given by,

$$U(r) = -\frac{GM}{f_1 r} - \frac{\delta_1(t) e^{-r\sqrt{-\xi}}}{6\xi r}, \quad (5)$$

where $\Lambda = 0$ assumed. However it is possible to consider cosmological constant Λ as dark energy to find the effect of dark energy on the cluster of galaxies (Hameeda et al. 2016a). In that case the effect of dynamical dark energy on the cluster of galaxies (Pourhassan et al. 2017) can be modeled using varying Λ or G (Kahya et al. 2015). Gravitational potential (4) corresponds to the following potential energy,

$$\Phi(r) = -\frac{GM^2}{f_1 r} - \frac{M\delta_1(t) e^{-r\sqrt{-\xi}}}{6\xi r}. \quad (6)$$

The thermodynamics applies as a description of various dynamical system on a macroscopic level with both equilibrium and non-equilibrium states. The argument for validity for non-equilibrium systems is that the globally averaged thermodynamical quantities like pressure, temperature, density and internal energy change more slowly than completely specified local configurations of particles. In gravitating N -body systems no rigorous equilibrium is possible because the gravitation is a long range force and does not saturate. Thus, the system of galaxies can be approximated as particles with pairwise interaction.

In order to study the thermodynamics of N particles or galaxies with equal mass M interacting gravitationally

with a potential energy $\Phi(r)$ given by (6), momenta p_i and average temperature T , the partition function is given by,

$$Z(T, V) = \frac{1}{\lambda^{3N} N!} \int d^{3N} p d^{3N} r \times \exp\left(-\left[\sum_{i=1}^N \frac{p_i^2}{2M} + \Phi(r)\right] T^{-1}\right), \quad (7)$$

where $N!$ corresponds to the distinguishability of classical particles, and λ takes care of the normalization factor resulting from integration over momentum space. Upon integration over momentum space, this reduces to

$$Z_N(T, V) = \frac{1}{N!} \left(\frac{2\pi MT}{\lambda^2}\right)^{3N/2} Q_N(T, V), \quad (8)$$

where the configurational integral, $Q_N(T, V)$, is given by

$$Q_N(T, V) = \int \dots \int \prod_{1 \leq i < j \leq N} \exp\left[-\frac{\phi(r_{ij})}{T}\right] d^{3N} r. \quad (9)$$

Here, the sum of the potential energies of all pairs is a function of the relative position vector $r_{ij} = |r_i - r_j|$ and corresponds $\sum_{1 \leq i < j \leq N} \phi(r_{ij}) = \Phi(r)$.

The configurational integral in terms of two particles function can be expressed as (Ahmad et al. 2002)

$$Q_N(T, V) = \int \dots \int \left[(1 + f_{12})(1 + f_{13})(1 + f_{23}) \dots (1 + f_{N-1, N}) \right] d^3 r_1 d^3 r_2 \dots d^3 r_N, \quad (10)$$

where two particles function has following form:

$$f_{ij} = e^{-\Phi(r_{ij})/T} - 1. \quad (11)$$

Here we note that the appearance of two particles function confirms the presence of interactions in the system and vanishes in absence of interactions.

At the cosmological scale we consider galaxies as a point particles, and in this approximation, the Hamiltonian and, therefore, the partition function of the systems diverge at $r_{ij} = 0$. In order to overcome this divergence, we consider the extended nature of particles (for example theory of infinitely extended particles of (Ahmad 1987) which reconsidered recently (Hameeda et al. 2016a)) by introducing a softening parameter which takes care of the finite size of each galaxy.

By introducing the softening parameter ϵ , the $f(R)$ modified gravitational (interaction) potential energy between particles which given by the equation (6) becomes

$$\Phi(r) = -\frac{GM^2}{f_1(r^2 + \epsilon^2)^{1/2}} - \frac{M\delta_1(t)e^{-r\sqrt{-\xi}}}{6\xi(r^2 + \epsilon^2)^{1/2}}. \quad (12)$$

The two particle function corresponding to the potential energy (12) has the following form:

$$f_{ij}(r) = \exp\left[\frac{GM^2}{f_1(r^2 + \epsilon^2)^{1/2}T} + \frac{M\delta_1(t)e^{-r\sqrt{-\xi}}}{6\xi(r^2 + \epsilon^2)^{1/2}T}\right] - 1. \quad (13)$$

As the system is moderately dilute, we can ignore higher order terms of the two particle function f_{ij} as

$$f_{ij}(r) = \left[\frac{GM^2}{f_1(r^2 + \epsilon^2)^{1/2}T} + \frac{M\delta_1(t)e^{-r\sqrt{-\xi}}}{6\xi(r^2 + \epsilon^2)^{1/2}T}\right]. \quad (14)$$

The configuration integrals over a spherical volume of radius R_1 for $N = 1$ yields,

$$Q_1(T, V) = V. \quad (15)$$

Moreover, the configuration integral $Q_2(T, V)$ for $N = 2$ has the following form:

$$Q_2(T, V) = 4\pi V \int_0^{R_1} \left[1 + \frac{GM^2}{f_1(r^2 + \epsilon^2)^{1/2}T} + \frac{M\delta_1(t)e^{-r\sqrt{-\xi}}}{6\xi(r^2 + \epsilon^2)^{1/2}T} \right] r^2 dr. \quad (16)$$

This further simplifies to

$$Q_2(T, V) = V^2 \left[1 + \frac{3GM^2}{2R_1T} \left(\frac{1}{f_1} \sqrt{1 + \frac{\epsilon^2}{R_1^2}} + \frac{\epsilon^2}{f_1 R_1^2} \log \frac{\epsilon/R_1}{\left[1 + \sqrt{1 + \frac{\epsilon^2}{R_1^2}}\right]} + \frac{\delta_1(t)}{147GM\xi} \left[\sqrt{1 + \frac{\epsilon^2}{R_1^2}} \left(-16R_1\sqrt{-\xi} + 32\frac{\epsilon^2}{R_1}\sqrt{-\xi} \left(1 - \frac{\epsilon/R_1}{\left[1 + \sqrt{1 + \frac{\epsilon^2}{R_1^2}}\right]} \right) - 6R_1^2\xi + 3(8 + 3\epsilon^2\xi) \right) + 3\frac{\epsilon^2}{R_1^2}(8 + 3\epsilon^2\xi) \log \frac{\epsilon/R_1}{\left[1 + \sqrt{1 + \frac{\epsilon^2}{R_1^2}}\right]} \right] \right] \right]. \quad (17)$$

If we define the dimensional quantities as

$$\alpha_1 = \sqrt{1 + \frac{\epsilon^2}{R_1^2}} + \frac{\epsilon^2}{R_1^2} \log \frac{\epsilon/R_1}{\left[1 + \sqrt{1 + \frac{\epsilon^2}{R_1^2}}\right]}, \quad \alpha_2 = \frac{\delta_1(t)}{147GM\xi} \left[\sqrt{1 + \frac{\epsilon^2}{R_1^2}} \left(-16R_1\sqrt{-\xi} + 32\frac{\epsilon^2}{R_1}\sqrt{-\xi} \left(1 - \frac{\epsilon/R_1}{\left[1 + \sqrt{1 + \frac{\epsilon^2}{R_1^2}}\right]} \right) - 6R_1^2\xi + 3(8 + 3\epsilon^2\xi) \right) + 3\frac{\epsilon^2}{R_1^2}(8 + 3\epsilon^2\xi) \log \frac{\epsilon/R_1}{\left[1 + \sqrt{1 + \frac{\epsilon^2}{R_1^2}}\right]} \right], \quad (18)$$

then, $Q_2(T, V)$ reduces to following compact form:

$$Q_2(T, V) = V^2 \left[1 + \frac{3}{2} \left(\frac{\alpha_1}{f_1} + \alpha_2 \right) \left(\frac{GM^2}{R_1T} \right)^3 \right]. \quad (19)$$

The following scale transformations of quantity: $\rho \rightarrow \lambda^{-3}\rho$, $T \rightarrow \lambda^{-1}T$ and $R_1 \rightarrow \lambda R_1$ leads to $\frac{GM^2}{R_1T} \rightarrow \left(\frac{GM^2}{R_1T}\right)^3 = \frac{3}{2} \left(\frac{GM^2}{T}\right)^3 \rho \equiv x$. With this, equation (19) reduces to

$$Q_2(T, V) = V^2(1 + \alpha x), \quad (20)$$

where

$$\alpha \left(\frac{\epsilon}{R_1} \right) = \frac{\alpha_1}{f_1} + \alpha_2. \quad (21)$$

For the point masses (i.e., $\epsilon = 0$), α reduces to

$$\alpha(\epsilon = 0) = 1 + \alpha_2|_{\epsilon=0}, \quad (22)$$

where

$$\alpha_2|_{\epsilon=0} = \frac{\delta_1(t)}{147GM\xi} \left[\left(-16R_1\sqrt{-\xi} - 6R_1^2\xi + 24 \right) \right]. \quad (23)$$

In same fashion, the configurational integrals for $N = 3, 4$ are obtained iteratively as

$$Q_3(T, V) = V^3(1 + \alpha x)^2, \quad (24)$$

and

$$Q_4(T, V) = V^4(1 + \alpha x)^3. \quad (25)$$

This enables us to write the most general form of configurational integral as

$$Q_N(T, V) = V^N(1 + \alpha x)^{N-1}. \quad (26)$$

Exploiting definition (8), we can write explicit form of the gravitational partition function for gravitating system under $f(R)$ gravity as

$$Z_N(T, V) = \frac{1}{N!} \left(\frac{2\pi MT}{\lambda^2} \right)^{3N/2} V^N (1 + \alpha x)^{N-1}. \quad (27)$$

Here, the correction due to $f(R)$ term is embedded in parameter α .

The possibility to eventually estimate the constraints for $f(R)$ theories which are in literature on the parameter α is made difficult by many factors. First of all, in a background analysis we generally don't need to define parameters like δ_1 , which is functional to the gravitational potential, but not to other cosmological quantities. The departure from general relativity is generally ascribed to the parameter $f_R \equiv df/dR$ which is almost equivalent to our f_1 , stated that most of the constraints on f_R are obtained assuming a model with $R + f(R)$. Thus, our $f_1 \sim 1$ would correspond to $f_R \sim 0$. One of the latest analysis of one of the most used models in literature, the Hu-Sawicki model (Hu & Sawicki 2007), gives an upper limit $|f_R| \lesssim 10^{-3}$, using dynamical probes (growth of matter perturbations and CMB power spectra data, among others) (Hu et al. 2016). This means that $f_1 \lesssim 1$ (because f_R from that analysis is negative) and, thus, makes a negligible contribution to α through the term α_1/f_1 .

Unfortunately, we cannot investigate the influence on α from δ_1 because the potential written as in Eq. (12) has not been studied extensively in literature. A similar, but not equivalent version of it, can be found in (Capozziello et al. 2009), but also in this case the parameter δ_1 was not explicitly left free in the analysis.

3 EQUATIONS OF STATE

Our goal of this section is to study the effects of $f(R)$ gravity on various thermodynamical equations of state of the theory. Once we have explicit expression for gravitational partition function is known, it is matter of calculation to derive various thermodynamical entities. For instance, with the help of relation between partition function and Helmholtz free energy as $F = -T \ln Z_N(T, V)$, we can derive Helmholtz free

energy as

$$F = -T \ln \left(\frac{1}{N!} \left(\frac{2\pi MT}{\lambda^2} \right)^{3N/2} V^N (1 + \alpha x)^{N-1} \right). \quad (28)$$

This further simplifies to

$$\begin{aligned} F &= NT \ln \left(\frac{N}{V} T^{-3/2} \right) - NT - (N-1)T \ln(1 + \alpha x) \\ &\quad - \frac{3}{2} NT \ln \left(\frac{2\pi M}{\lambda^2} \right). \end{aligned} \quad (29)$$

In the Fig. 1 and Fig. 2 we can see behavior of the Helmholtz free energy in terms of N with variation of $\delta_1(t)$ (Fig. 1) and ϵ (Fig. 2). It is illustrated that there is a minimum for Helmholtz free energy. We show that both parameter enhanced Helmholtz free energy. It means that modified gravity correction increases value of the Helmholtz free energy. For the enough large $\delta_1(t)$ the value of the Helmholtz free energy is positive. Hence, if $\delta_1(t)$ be increasing function of time, hence Helmholtz free energy is increasing function of time (later with analyze of the entropy we show that $\delta_1(t)$ must be increasing function of time). We also find that Helmholtz free energy corresponding to point masses is smaller than Helmholtz free energy corresponding to the extended masses. Moreover, by the red lines of the Fig. 2 (lower lines) we can see that effects of modified gravity (comparison with standard general relativity) is increasing of Helmholtz free energy. This point deserves some comments. As we have shown, the Helmholtz free energy is a quantity depending on α , and α depends on ϵ . As ϵ is a parameter introduced to take into account extended structures, the Helmholtz free energy results different with respect to that of point-like masses. In our specific case, improving ϵ gives rise to the improvement of the Helmholtz free energy. From a physical point of view, this means that the Helmholtz free energy depends on the size of the system (the size of the galaxy) and the interaction potential, (here a Newtonian potential corrected with a Yukawa term). Being such a free energy an *extensive* thermodynamical quantity, depending on the volume, it is obviously larger than that of a point-like system.

Since entropy S and Helmholtz free energy are related with the following formula: $S = - \left(\frac{\partial F}{\partial T} \right)_{N,V}$. Hence, corresponding to Helmholtz free energy (29), the entropy is given by,

$$\begin{aligned} S &= N \ln \left(\frac{V}{N} T^{3/2} \right) + (N-1) \ln(1 + \alpha x) \\ &\quad - 3N \frac{\alpha x}{1 + \alpha x} + \frac{5}{2} N + \frac{3}{2} N \ln \left(\frac{2\pi M}{\lambda^2} \right). \end{aligned} \quad (30)$$

Here we note that N is large enough to assume $N-1 \approx N$. This leads to following specific entropy:

$$\frac{S}{N} = \frac{S_0}{N} - 3 \frac{\alpha x}{1 + \alpha x} + \ln \left(\frac{V}{N} T^{3/2} \right) - \ln \left(1 - \frac{\alpha x}{1 + \alpha x} \right), \quad (31)$$

where $S_0 = \frac{5}{2} N + \frac{3}{2} N \ln \left(\frac{2\pi M}{\lambda^2} \right)$. These expressions coincide with their standard form (Ahmad et al. 2002) except the modification in the form of clustering parameter of galaxies, \mathcal{B} , defined as

$$\mathcal{B} = \frac{\alpha x}{1 + \alpha x}. \quad (32)$$

Here, we note that the form of the modified clustering parameter emerges naturally. The clustering parameter is an

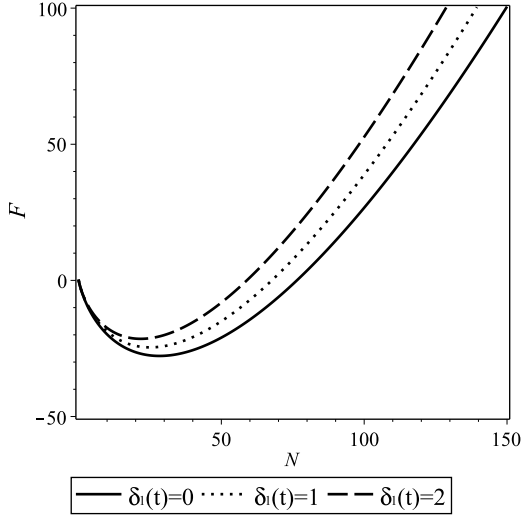


Figure 1. Typical behavior of the Helmholtz free energy in terms of N with variation of $\delta_1(t)$. We set unit value for all other parameters.

important quantity because its value governs the strength of clustering.

In case of point masses, i.e. $\epsilon = 0$, the modified clustering parameter under $f(R)$ gravity takes the following form:

$$\mathcal{B}(\epsilon = 0) := \mathcal{B}_0 = \frac{(1 + \alpha_2|_{\epsilon=0})x}{1 + x(1 + \alpha_2|_{\epsilon=0})}. \quad (33)$$

In the Fig. 3 we can see behavior of the entropy with modified gravity parameter $\delta_1(t)$. It is clear that if $\delta_1(t)$ be increasing function of time, then the entropy is also increasing function of time in agreement with the second law of the thermodynamics. We also can see that the entropy of the point masses diverges after the entropy of the extended masses. In order to have comparison with standard general relativity one can take $\xi \rightarrow \infty$ limit and obtain red (three lines in right) lines of the Fig. 3. We can see similar behavior in general but with different asymptotic points. Also in the case of $\delta_1(t) \rightarrow 0$ both have similar behavior as expected.

Since the explicit forms of Helmholtz free energy and entropy are known, therefore the form of internal energy, U , can be easily derived with the help of definition, $U = F + TS$, as

$$U = \frac{3}{2}NT(1 - 2\mathcal{B}). \quad (34)$$

The form of internal energy coincides with the standard form. However, corrections due to $f(R)$ gravity is embedded in clustering parameter \mathcal{B} . In the Fig. 4 we can see general behavior of the internal energy in the modified gravity (solid line) and standard general relativity (dashed line). We can see that the effect of modified gravity is increasing of the internal energy.

The pressure, P and chemical potential, μ , are related with Helmholtz free energy as $P = -\left(\frac{\partial F}{\partial V}\right)_{N,T}$ and

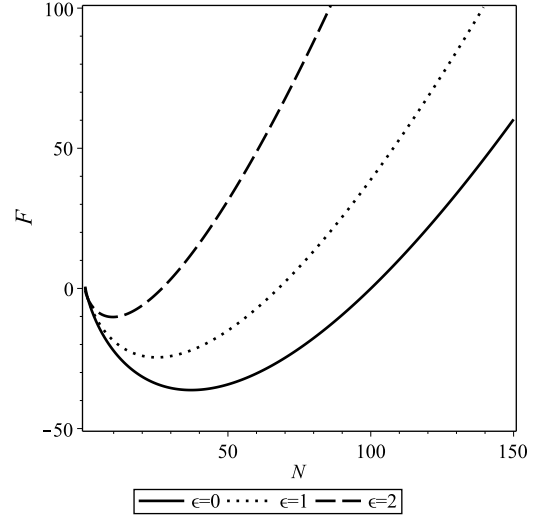


Figure 2. Typical behavior of the Helmholtz free energy in terms of N with variation of ϵ . Black lines are corresponding to modified gravity while red lines are corresponding to standard general relativity. We set unit value for all other parameters.

$\mu = \left(\frac{\partial F}{\partial N}\right)_{V,T}$, respectively. Therefore, the explicit form of pressure and chemical potential can be given as

$$P = \frac{NT}{V}(1 - \mathcal{B}), \quad (35)$$

$$\begin{aligned} \mu &= T \ln \left(\frac{N}{V} T^{-3/2} \right) + T \ln(1 - \mathcal{B}) \\ &\quad - \frac{3}{2}T \ln \left(\frac{2\pi M}{\lambda^2} \right) - \mathcal{B}T. \end{aligned} \quad (36)$$

These expressions also coincide with their standard forms. The only difference is the value of clustering parameter which exhibits correction due to the $f(R)$ gravity. This chemical potential can be utilized to study the distribution function of the system. We find that both P and μ behave similar internal energy hence the effect of modified gravity is increasing of the pressure and chemical potential.

4 GENERAL DISTRIBUTION FUNCTION

Here, we assume that the system of galaxy is in quasi-equilibrium and follows grand canonical ensemble. For grand canonical ensemble, the partition function is defined by

$$Z_G(T, V, z) = \sum_{N=0}^{\infty} z^N Z_N(V, T), \quad (37)$$

where z refers to absolute activity. The grand partition function for the system of galaxies interacting through $f(R)$ gravity is given by

$$\ln Z_G = \frac{PV}{T} = N(1 - \mathcal{B}). \quad (38)$$

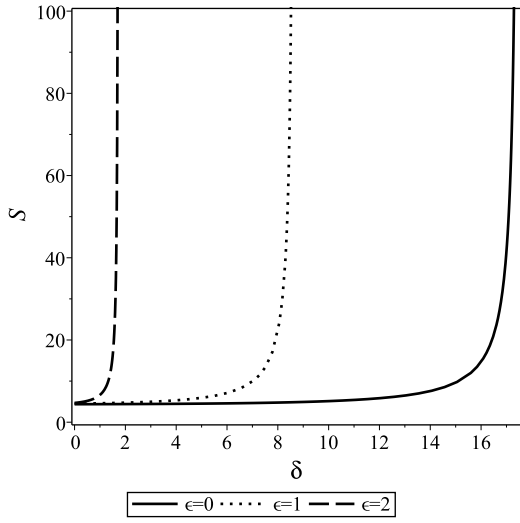


Figure 3. Typical behavior of the entropy in terms of $\delta_1(t)$ by variation of ϵ . We set unit value for all other parameters.

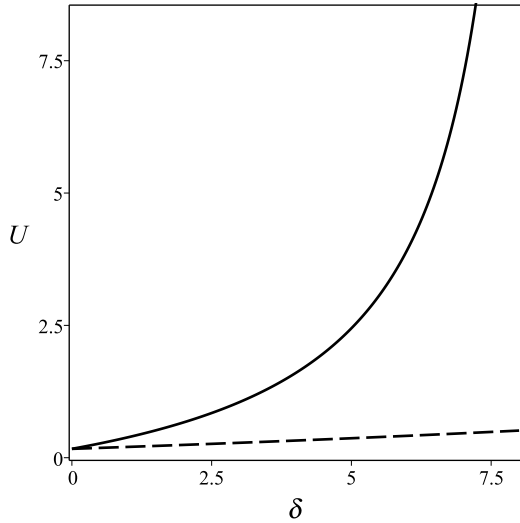


Figure 4. Typical behavior of the internal energy in terms of $\delta_1(t)$ for modified gravity (solid line) and standard general relativity (dashed line) We set unit value for all parameters.

For a statistical system, the distribution function (probability of finding N particles in volume V) is given by

$$p_V(N) = \frac{\sum_i e^{\frac{N\mu}{T}} e^{\frac{-U_i}{T}}}{Z_G(T, V, z)} = \frac{e^{\frac{N\mu}{T}} Z_N(V, T)}{Z_G(T, V, z)}. \quad (39)$$

Exploiting relation (38), the distribution function of gravitational system with extended mass interacting under $f(R)$

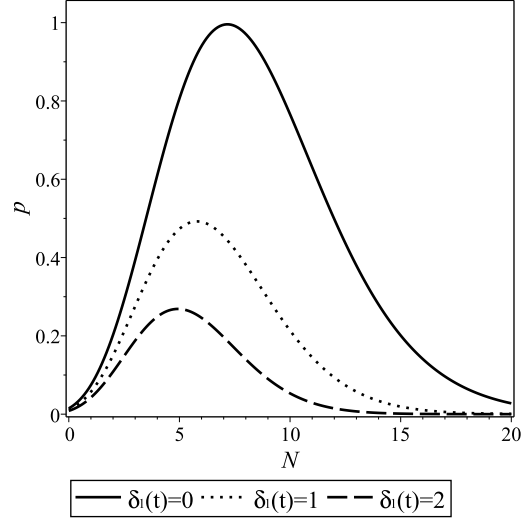


Figure 5. Typical behavior of the distribution function in terms of N by variation of $\delta_1(t)$. We set unit value for all other parameters.

gravity is given by

$$p_V(N, \epsilon) = \frac{\bar{N}^N}{N!} \left(1 + \frac{N}{\bar{N}} \frac{\mathcal{B}}{(1-\mathcal{B})}\right)^{N-1} \times \left(1 + \frac{\mathcal{B}}{(1-\mathcal{B})}\right)^{-N} e^{[-N\mathcal{B} - \bar{N}(1-\mathcal{B})]}. \quad (40)$$

For point mass case, i.e. $\epsilon = 0$, the expression of distribution function reads,

$$p_V(N, \epsilon = 0) = \frac{\bar{N}^N}{N!} \left(1 + \frac{N}{\bar{N}} \frac{\mathcal{B}_0}{(1-\mathcal{B}_0)}\right)^{N-1} \times \left(1 + \frac{\mathcal{B}_0}{(1-\mathcal{B}_0)}\right)^{-N} e^{[-N\mathcal{B}_0 - \bar{N}(1-\mathcal{B}_0)]}. \quad (41)$$

From the above expression, it is evident that, beside the expression of clustering parameter \mathcal{B} , the form of distribution function exactly matches with their standard form given in Ref. (Ahmad et al. 2002). The form of standard clustering parameter, b , is given by,

$$b = \frac{x}{1+x}, \quad (42)$$

which is clearly different than the our clustering parameter (32). In the Fig. 5 we draw distribution function (40) in terms of N and see that probability of finding N particles in volume V in the modified gravity $\delta_1(t) \neq 0$ is smaller than the case of $\delta_1(t) = 0$. It is the case because total volume in modified gravity is bigger than the case in standard general relativity, and it is clear for example from the equation (??). Easily by taking $\xi \rightarrow \infty$ limit one can obtain standard general relativity probability which is higher than the case of modified gravity.

5 CRITICAL TEMPERATURE

In this section, we study the stability and critical temperature of the galaxy clustering. The specific heat and their variation for perfect gas to virialized gas ($\mathcal{B} = 1$) have illuminating physical insights into clustering. The expression of specific heat at constant volume is given by

$$C_V = \frac{1}{N} \left(\frac{\partial U}{\partial T} \right)_{N,V} = \frac{3}{2} \left[\frac{1 + 6\alpha x - 4\alpha^2 x^2}{(1 + \alpha x)^2} \right]. \quad (43)$$

It can be clearly seen from the expression that in the limit $\alpha \rightarrow 0$ (and hence $\mathcal{B} \rightarrow 0$), the specific heat at constant volume reduces to $C_V = 3/2$. This means that in this limit system behaves a monotonic perfect gas system. On the other hand, for completely virialized system where galaxies are strongly clustered, (i.e., $\alpha x \rightarrow \infty$ or $\mathcal{B} = 1$), the specific heat takes following value:

$$C_V = -\frac{3}{2}. \quad (44)$$

The negative value of specific heat signifies that the system is unstable. Here, we note that the instability of system of galaxies are not analogous to the system of imperfect gases as gravitating systems contribute extra degrees of freedom due to semistability. The negative specific heat can be justified as suppose many galaxies attach to clusters and therefore impart energy to clusters which causes galaxies to rise out of cluster potential wells. Consequently, galaxies lose kinetic energy and become cooler, therefore producing the negative overall value of specific heat. Moreover, in limit $\alpha x \rightarrow \frac{1}{2}$, the specific heat of the system reduces to

$$C_V = \frac{5}{2}, \quad (45)$$

which shows the behavior of diatomic gas. By maximizing C_V with temperature, i.e.,

$$\frac{\partial C_V}{\partial T} = 0, \quad (46)$$

we can get the value of critical temperature.

The critical temperature for point structured galaxies is obtained as

$$T_c(\epsilon = 0) = \left[3 \frac{\bar{N}}{V} (GM^2)^3 (1 + \alpha_2|_{\epsilon=0}) \right]^{1/3}. \quad (47)$$

For extended structure galaxies, the expression of critical temperature is

$$T_c = \left[3 \frac{\bar{N}}{V} (GM^2)^3 (\alpha_1 + \alpha_2) \right]^{1/3}, \quad (48)$$

where parameter α_1 and α_2 have explicit expressions in (18).

The specific heat for both point and extended mass cases can be expressed in terms of critical temperature as

$$C_V = \frac{3}{2} \left[1 - 2 \frac{1 - 4 \left(\frac{T}{T_c} \right)^3}{\left(1 + 2 \left(\frac{T}{T_c} \right)^3 \right)^2} \right]. \quad (49)$$

The above form coincides exactly with the the form given in Ref. (Saslaw & Ahmad 2010). This justifies the claim even in $f(R)$ case that at critical temperature the basic homogeneity of the system has been broken on the average interparticle

scale by the formation of binary systems bounded gravitationally. We express the clustering parameter in terms of critical temperature as

$$\mathcal{B} = \frac{T_c^3}{T_c^3 + 2T^3}. \quad (50)$$

This implies that, at critical temperature, i.e. $T = T_c$, the corrected clustering parameter takes following value: $\mathcal{B}_{crit} = 1/3$. We can call this as a critical value of clustering parameter at which the specific heat takes its maximum value.

The pressure and internal energy can be expressed in terms of critical temperature as following:

$$P = \frac{2N}{V} \left(\frac{T^4}{T_c^3 + 2T^3} \right), \quad (51)$$

$$U = \frac{3}{2} NT \left(\frac{2T^3 - T_c^3}{2T^3 + T_c^3} \right). \quad (52)$$

It is evident that at critical temperature, i.e. $T = T_c$, the pressure and internal energy take following values: $P = \frac{2}{3} \frac{NT}{V}$ and $U = \frac{1}{2} NT$, respectively.

6 THE GALAXY-GALAXY CORRELATION FUNCTION IN $F(R)$ GRAVITY

In this section, we would like to examine the behavior of two particle correlation function under the effect of $F(R)$ gravity. In fact, the power law behavior of two particle correlation function $\Xi(x)$ in clustering of galaxies, i.e. $\Xi(x) = r^{-1.8}$, has been established by observation (Peebles 1980) as well as by N -body simulation (Suto et al. 1990).

The internal energy U for a system of spherical volume V consisting of N -particles has following form (Saslaw 2000):

$$U = \frac{3}{2} NT - \frac{N\rho}{2} \int_V \Phi(r) \Xi(r) 4\pi r^2 dr, \quad (53)$$

where interaction potential between two galaxies Φ in $f(R)$ gravity is given in Eq. (12). Now, in order to see the modification in the power law of correlation function, the clustering parameter is defined as

$$\mathcal{B} = \frac{GM^2 \rho}{6T} \int \frac{r \Xi(r)}{\sqrt{\epsilon^2 + r^2}} \left(\frac{1}{f_1 r} + \frac{\delta_1(t) e^{-r\sqrt{-\xi}}}{6GM\xi} \right) dV. \quad (54)$$

The volume differentiation of this yields following expression:

$$\begin{aligned} \frac{\partial \mathcal{B}}{\partial V} &= \frac{Gm^2 \rho}{6T} \frac{d\rho}{dV} \int \frac{r \Xi(r)}{\sqrt{\epsilon^2 + r^2}} \left(\frac{1}{f_1 r} + \frac{\delta_1(t) e^{-r\sqrt{-\xi}}}{6GM\xi} \right) dV \\ &+ \frac{Gm^2 \rho}{6T} \frac{\partial}{\partial V} \int \frac{r \Xi(r)}{\sqrt{\epsilon^2 + r^2}} \left(\frac{1}{f_1 r} + \frac{\delta_1(t) e^{-r\sqrt{-\xi}}}{6GM\xi} \right) dV. \end{aligned} \quad (55)$$

Inserting following relation

$$\frac{\partial \mathcal{B}}{\partial V} = \frac{\partial \rho}{\partial V} \frac{\partial \mathcal{B}}{\partial \rho} \quad (56)$$

in Eq. (55), we get

$$\frac{\partial \mathcal{B}}{\partial \rho} = \frac{\mathcal{B}(1 - \mathcal{B})}{\rho}. \quad (57)$$

Since $\rho = \frac{N}{V}$, therefore

$$\frac{\partial \rho}{\partial V} = -\frac{\rho}{V}. \quad (58)$$

Upon further simplifications of above relations, we get the following functional form of correlation function:

$$\xi(r) = \frac{9\mathcal{B}^2 T}{2\pi G m^2 \rho} \frac{1}{r^2} \left(1 + \frac{\epsilon^2}{2r^2}\right) \left(\frac{1}{f_1 r} + \frac{\delta_1(t) e^{-r\sqrt{-\xi}}}{6GM\xi}\right)^{-1}, \quad (59)$$

where we have neglected the higher powers of ϵ/r . From relation (59), the effects of $f(R)$ modifications to the correlation function can be easily seen. First of all, we notice how f_1 would only change the amount of correlation (the larger f_1 , the larger ξ), but not the radial behavior; instead, δ_1 has a twofold effect, both on the degree of correlation (the larger δ_1 , the smaller ξ) and on the radial dependence through the exponential behaviour. Finally, as explained in the previous sections, it is not easy to quantify and convert present constraints on $f(R)$ in terms of changes in the correlation function, due to the variety of $f(R)$ models which are considered, and to the chosen theoretical parameters.

7 OBSERVATIONAL DATA

In order to test the feasibility of an $f(R)$ -gravity approach to the clustering of galaxies using some of the tools developed in the previous sections, we need to choose a galaxy and/or cluster catalog to be compared with theory. We have chosen to work with the cluster catalog described in (Wen & Han 2012), containing 132, 684 clusters of galaxies in the redshift range $0.05 \leq z < 0.8$. The catalogue is based on the identification of clusters and groups of galaxies from the Sloan Digital Sky Survey III (SDSS-III). Even if there is a more updated version of the same catalogue (Wen & Han 2015), we have decided to work with this older version because it provides, for each cluster, all the quantities we need to test our theory by using Eq. (40). In particular, among others, the catalogue provides:

- the radius of the cluster, r_{200} in *Mpc*, which is, as usual, the radius within which the mean density of a cluster is 200 times the critical density of the universe at the same redshift;
- N_{200} , the number of member galaxy candidates for each given cluster, within r_{200} .

The most recent version of the same catalogue (Wen & Han 2015) provides slightly more accurate estimations for clusters' masses, but at $r_{500} < r_{200}$; as we are not interested in masses, but only in galaxy counts-in-cells, and we want to explore the largest volumes possible, we will stick to the older numbers from (Wen & Han 2012), even if a comparison between the clustering at r_{500} and at r_{200} might be interesting. But we will leave it for future works.

How do we perform the counts-in-cell procedure? First, we identify the cells with the volumes corresponding to each r_{200} ; thus, for us, each cluster in the catalogue is a properly defined cell. Then, for each cluster/cell, we derive the observed distribution function $p_V(N)$ by counting how many galaxies are in each cell, i.e., by using the given N_{200} data. Considering that we are given both the redshift z and the radius r_{200} for each cluster, we divide the full sample in smaller groups and try to detect, if any, a possible dependence of the theoretical parameters with scale and time. We have divided the total sample in redshift bins with width $\Delta z = 0.05$, and radius bins with width $\Delta r_{200} = 0.1$ *Mpc*. From the

obtained sub-groups, we have selected only those containing a sufficiently large number of clusters, ending with the groups corresponding to cell/cluster radii $0.8 < r_{200} < 0.9$, $0.9 < r_{200} < 1.0$ and $1.0 < r_{200} < 1.1$ *Mpc*, and to redshift $0.05 \leq z \leq 0.65$. We need to remember that the catalogue we are using is complete up to a redshift $z \sim 0.42$, for clusters with an estimated mass $M_{200} > 1 \cdot 10^{14} M_\odot$; at higher redshift, a bias toward smaller clusters (lower masses) is possible (Wen & Han 2012).

It is important to highlight here some main differences between the way we perform our counts-in-cells analysis and previous works in literature. In most of the latter ones (Rahmani et al. 2009; Sivakoff & Saslaw 2005), once a catalogue is chosen, the covered sky is divided in cells by fixing their angular dimensions, and the galaxy count is performed in each cell for each chosen angle. These counts are then compared with the theoretical expectation for the distribution function $p_V(N)$. Instead, we follow more closely the approach of (Yang & Saslaw 2011, 2012), where the cells are determined by their physical length, in our case the radius r_{200} . This latter approach has also another benefit which becomes more important and evident when working with a sample which extends on a large redshift interval, like in our case: the same physical length is used as reference cell radius at every redshift, while the former approach, with the cells being determined by constant angular dimensions, would imply that larger physical cells/volumes are explored at higher redshift with respect to lower redshift ones.

Another maybe even more important difference, however, is in the way the cells are defined. All the former references start from a galaxy sample, define a cell volume, and cover the full sky by this mapping; then, galaxies are counted in each cell but without taking into consideration the *clustering status* of the galaxies, i.e., if they form structures (groups and clusters) or if they are field galaxies. What is generally argued, is that the cell radius, at least numerically, *could* correspond to a cluster and/or group of galaxies scale, but there is no certainty that such structures are present and no correspondence is looked for concerning this aspect. In (Wen & Han 2012), the galaxy catalog from SDSS-III is scanned exactly for this purpose, namely, to search for groups and clusters of galaxies, and is eventually returned as a cluster catalog. Thus, we will explore the compatibility of the theoretical distribution function with consistently-identified clustered structures. This same analysis has been started for the first time in (Yang & Saslaw 2012), but on a much smaller redshift range than that we consider in this work. Also, as we are working on scales which are much smaller than those where the quasi-equilibrium clustering should be more effective, there will be some consequences and caveats which we will have to take in mind when interpreting our results, as explained in (Yang & Saslaw 2011, 2012).

In Table 1 we report results from fitting Eq. (40) with the chosen cluster catalog data. The parameters involved in Eq. (40) are rewritten as:

- $R_1 = r_{200}$ is the volume radius of the cell (cluster) we have considered; as explained above, we bin the data with respect to R_1 ;
- $N = N_{200}$ is the number of galaxies in each cell/cluster;

Table 1. Results from fitting Eq. (40) with data from the cluster catalog from (Wen & Han 2012). Data and fits are divided in redshift bins (first column) and cell radius bin (as indicated by R intervals). N_{cl} is not a fitting parameter, but the number of clusters in each redshift and radius bin. All the fitting parameters are described in the text.

z	χ^2_s						χ^2_s						χ^2_s					
	$0.8 < R_1 < 0.9 \text{ Mpc}$						$0.9 < R_1 < 1.0 \text{ Mpc}$						$1.0 < R_1 < 1.1 \text{ Mpc}$					
	N_{cl}	\bar{N}	b	\bar{L}	$\bar{\delta}_1$	f_1	N_{cl}	\bar{N}	b	\bar{L}	$\bar{\delta}_1$	f_1	N_{cl}	\bar{N}	b	\bar{L}	$\bar{\delta}_1$	f_1
[0.05, 0.1]	291	$9.33^{+0.12}_{-0.13}$	< 0.16	< 9.16	< 3.75	290	390	$11.16^{+0.19}_{-0.20}$	< 0.22	< 4.43	< 6.38	2955	298	$14.04^{+0.09}_{-0.09}$	< 0.10	< 1.11	162	4.99
[0.1, 0.15]	1052	$10.01^{+0.15}_{-0.15}$	$0.069^{+0.056}_{-0.056}$	< 1.20	< 125	191	1526	$11.96^{+0.10}_{-0.10}$	< 0.16	< 2.14	< 28.1	0.33	949	$15.59^{+0.05}_{-0.05}$	< 0.19	< 2.96	< 2.44	60.9
[0.15, 0.2]	2343	$10.54^{+0.16}_{-0.17}$	< 0.23	< 4.01	< 11.1	18	2919	$12.93^{+0.11}_{-0.10}$	< 0.21	< 5.71	< 3.12	97.3	1826	$16.75^{+0.03}_{-0.03}$	$0.05^{+0.20}_{-0.04}$	$0.47^{+0.44}_{-0.27}$	< 18.6	53.6
[0.2, 0.25]	3069	$10.58^{+0.14}_{-0.14}$	< 0.26	< 4.91	< 6.43	4219	3688	$12.85^{+0.05}_{-0.05}$	< 0.094	< 1.24	< 67.8	165	2398	$16.92^{+0.07}_{-0.07}$	$0.076^{+0.069}_{-0.057}$	< 0.93	25.7	335
[0.25, 0.3]	3318	$10.13^{+0.14}_{-0.14}$	< 0.16	< 1.68	< 70.6	2716	3982	$12.56^{+0.15}_{-0.15}$	< 0.25	< 4.21	< 4.93	27.2	2443	$16.17^{+0.10}_{-0.10}$	< 0.16	< 4.33	< 5.71	88.9
[0.3, 0.35]	4024	$10.28^{+0.14}_{-0.14}$	< 0.096	< 1.36	< 148	905	5055	$12.48^{+0.15}_{-0.15}$	< 0.13	< 1.39	< 56.5	182	2958	$16.35^{+0.13}_{-0.13}$	< 0.20	< 2.82	< 8.17	39.9
[0.35, 0.4]	4379	$10.36^{+0.14}_{-0.14}$	< 0.22	< 6.63	< 4.95	0.26	5402	$12.70^{+0.16}_{-0.15}$	< 0.098	< 1.01	15.0	90.0	3208	$16.37^{+0.13}_{-0.13}$	< 0.19	< 2.10	< 11.8	63.5
[0.4, 0.45]	4925	$10.09^{+0.18}_{-0.18}$	< 0.20	< 4.27	< 16.1	13.5	5819	$12.35^{+0.19}_{-0.18}$	< 0.13	< 1.21	< 96.3	17771	3289	$16.10^{+0.19}_{-0.19}$	< 0.13	< 2.59	< 26.9	218
[0.45, 0.5]	3982	$9.45^{+0.11}_{-0.12}$	< 0.15	< 0.59	< 216	554	4813	$11.38^{+0.17}_{-0.17}$	< 0.23	< 3.83	< 12.5	634	2660	$14.65^{+0.17}_{-0.17}$	< 0.08	< 0.81	< 171	131
[0.5, 0.55]	2838	$8.92^{+0.22}_{-0.21}$	< 0.18	< 2.91	< 34.3	35.9	3631	$10.15^{+0.14}_{-0.14}$	< 0.16	< 1.36	47.8	5450	2009	$12.98^{+0.15}_{-0.16}$	< 0.19	< 2.65	< 19.5	1594
[0.55, 0.6]	1971	$8.69^{+0.24}_{-0.25}$	< 0.11	< 1.48	< 201	3.39	2614	$9.61^{+0.34}_{-0.36}$	< 0.23	< 3.99	< 14.1	0.19	1538	$12.28^{+0.15}_{-0.15}$	< 0.20	< 3.60	< 8.23	119
[0.6, 0.65]	1046	$8.49^{+0.20}_{-0.21}$	< 0.29	< 4.47	< 8.30	215	1586	$9.26^{+0.32}_{-0.34}$	< 0.18	< 1.99	< 63.3	908	977	$11.18^{+0.18}_{-0.18}$	< 0.15	< 3.67	< 20.7	18.9

z	χ^2_k						χ^2_k						χ^2_k					
	$0.8 < R_1 < 0.9 \text{ Mpc}$						$0.9 < R_1 < 1.0 \text{ Mpc}$						$1.0 < R_1 < 1.1 \text{ Mpc}$					
	N_{cl}	\bar{N}	b	\bar{L}	$\bar{\delta}_1$	f_1	N_{cl}	\bar{N}	b	\bar{L}	$\bar{\delta}_1$	f_1	N_{cl}	\bar{N}	b	\bar{L}	$\bar{\delta}_1$	f_1
[0.05, 0.1]	291	$9.39^{+0.08}_{-0.08}$	< 0.20	< 1.95	< 36.6	$9.6 \cdot 10^5$	390	$11.26^{+0.07}_{-0.07}$	$0.04^{+0.10}_{-0.03}$	$0.48^{+0.49}_{-0.30}$	< 204	2791	298	$14.26^{+0.08}_{-0.08}$	< 0.13	$0.63^{+1.13}_{-0.42}$	< 8.57	$7.0 \cdot 10^5$
[0.1, 0.15]	1052	$10.15^{+0.04}_{-0.05}$	$0.13^{+0.15}_{-0.08}$	< 0.78	< 57.8	117	1526	$12.01^{+0.04}_{-0.04}$	< 0.15	< 0.98	< 35.6	1156	949	$15.55^{+0.04}_{-0.04}$	< 0.10	< 0.95	< 17.9	$7.4 \cdot 10^4$
[0.15, 0.2]	2343	$10.69^{+0.03}_{-0.03}$	< 0.24	< 1.39	< 25.1	2106	2919	$12.99^{+0.03}_{-0.03}$	< 0.11	< 1.02	< 62.1	31.7	1826	$16.81^{+0.04}_{-0.03}$	< 0.06	< 0.75	< 21.3	342
[0.2, 0.25]	3069	$10.57^{+0.07}_{-0.07}$	< 0.10	< 1.04	< 103	156	3688	$12.97^{+0.03}_{-0.03}$	< 0.16	< 0.99	< 29.6	705	2398	$16.94^{+0.03}_{-0.03}$	< 0.11	< 0.77	< 27.9	2673
[0.25, 0.3]	3318	$10.26^{+0.03}_{-0.03}$	$0.14^{+0.21}_{-0.09}$	< 0.84	< 61.2	956	3982	$12.59^{+0.03}_{-0.03}$	< 0.16	< 0.92	< 55.1	8.71	2443	$16.19^{+0.03}_{-0.03}$	< 0.08	< 0.99	< 50.4	152
[0.3, 0.35]	4024	$10.44^{+0.03}_{-0.03}$	< 0.25	< 1.81	< 24.0	116	5055	$12.55^{+0.03}_{-0.03}$	< 0.30	< 1.82	< 8.21	816	2958	$16.38^{+0.03}_{-0.03}$	< 0.20	< 0.68	< 29.8	146
[0.35, 0.4]	4379	$10.52^{+0.03}_{-0.03}$	$0.12^{+0.14}_{-0.07}$	< 0.72	< 74.3	63.6	5402	$12.75^{+0.02}_{-0.02}$	< 0.05	$2.73^{+4.62}_{-1.43}$	< 19.3	41.1	3208	$16.45^{+0.03}_{-0.03}$	< 0.19	< 0.86	< 23.0	11.6
[0.4, 0.45]	4925	$10.31^{+0.038}_{-0.03}$	< 0.29	< 3.08	23.4	54.8	5819	$12.45^{+0.02}_{-0.03}$	< 0.11	< 0.94	< 99.7	1067	3289	$16.08^{+0.03}_{-0.03}$	$0.12^{+0.16}_{-0.07}$	< 0.87	3.30	14.6
[0.45, 0.5]	3982	$9.78^{+0.03}_{-0.03}$	< 0.35	< 3.69	14.2	176	4813	$11.50^{+0.03}_{-0.03}$	< 0.19	< 1.02	< 50.8	817	2660	$14.69^{+0.03}_{-0.03}$	$0.15^{+0.20}_{-0.10}$	< 0.93	< 25.6	131
[0.5, 0.55]	2838	$9.25^{+0.03}_{-0.03}$	< 0.26	$4.66^{+5.22}_{-2.43}$	< 2.27	0.86	3631	$10.33^{+0.03}_{-0.03}$	$0.32^{+0.21}_{-0.15}$	< 0.99	< 15.9	52.7	2009	$13.0^{+0.03}_{-0.03}$	< 0.17	< 0.82	< 48.7	1201
[0.55, 0.6]	1971	$9.06^{+0.04}_{-0.04}$	< 0.25	< 3.45	< 12.2	2.08	2614	$10.37^{+0.05}_{-0.05}$	< 0.28	< 1.13	< 36.5	2443	1538	$12.38^{+0.05}_{-0.05}$	< 0.11	< 1.07	< 53.9	158
[0.6, 0.65]	1046	$8.85^{+0.05}_{-0.05}$	< 0.24	< 1.54	1.84	$1.4 \cdot 10^4$	1586	$9.50^{+0.05}_{-0.04}$	< 0.19	< 1.20	< 73.6	41.3	977	$11.32^{+0.05}_{-0.05}$	< 0.19	< 1.12	< 37.2	61.5

- the dimensionless softening parameter:

$$\tilde{\epsilon} = \frac{\epsilon}{R_1}; \quad (60)$$

- the interaction range of the $f(R)$ model, both dimensional (in Mpc):

$$L = \frac{1}{\sqrt{-\xi}} = \sqrt{-\frac{6f_2}{f_1}}; \quad (61)$$

and dimensionless:

$$\tilde{L} = \frac{L}{R_1}. \quad (62)$$

Thus, it is clear we leave \tilde{L} and f_1 as free parameters in our fitting procedure, while f_2 can be determined from them;

- the clustering parameter b , which enters Eq. (40) through:

$$\mathcal{B} = \frac{b\alpha}{1+b(\alpha-1)}; \quad (63)$$

- the dimensionless time-function parameter which quantify the deviation of the $f(R)$ -model from General Relativity

(GR):

$$\tilde{\delta}_1 = \frac{\delta_1 R_1^2}{GM}. \quad (64)$$

Note that in GR we have only two parameters for Eq. (40), i.e. \bar{N} and b which might be even derived directly from observations, if the counts-in-cells were performed on scales large enough for the quasi-equilibrium condition to hold. Thus, in principle, in GR, we would have no free parameters. However, it is also clear that if one wants to perform a fit of the same data with a given expression for the distribution function, a maximum of two free parameters are present. Then, it is obvious that for our $f(R)$ model, which has five free parameters (including the $f(R)$ parameters $\tilde{L}, \tilde{\delta}_1, f_1$), and given the way they enter in Eq. (40), we might have a lot of degeneracies in our case and very likely we won't be able to constrain in a statistically satisfying way most of the parameters. In Table 1 we also include N_{cl} , i.e. the number of clusters in each redshift bin, but this won't be a fitting parameter.

In order to fit the data, we have used two different ap-

proached. First, we have performed a proper least-square minimization, i.e. we minimize the quantity

$$\chi_{ls}^2 = \sum_i \left(p_V^{theo}(N_i) - p_V^{obs}(N_i) \right)^2, \quad (65)$$

where $p_V^{obs}(N_i)$ is the counts-in-cell distribution from data, and $p_V^{theo}(N_i)$ is the counts-in-cell expected from $f(R)$, as given in Eq. (40). The index i derives from the fact that in each bin, we have a minimal and maximum N_{200} ; we select i finite values in the range $[N_{min}, N_{max}]$ at which we evaluate the distribution function, both observational and theoretical. Second, we also perform a χ^2 -like analysis, minimizing the quantity:

$$\chi_{jk}^2 = \sum_i \frac{\left(p_V^{theo}(N_i) - p_V^{obs}(N_i) \right)^2}{\sigma_i^2}, \quad (66)$$

where σ_i are the errors on $p_V^{obs}(N_i)$. We have derived these errors from the data with a jackknife-like procedure. For each redshift and radius bin:

- (i) we cut a fraction \mathcal{F} from the total bin population;
- (ii) we derive the counts-in-cell distribution function for the cut sample, i.e. we have a new distribution for the N_i defined as above.

The previous steps are performed for different fraction \mathcal{F} , ranging from 10% to 90% of the total sample; and for each fraction, we repeat the same steps up to ~ 50 times. In such a way, we end up with a very-closely-gaussian distribution of $\sim 50 N_i$ (for each i) values; for each of them, we extract the standard deviation and assume this last quantity as the error σ_i . The data points and the errors so obtained are shown as black dots and bars in Figs. (6) - (7) - (8). The best fitting $p_V(N)$ distributions obtained from the minimization of χ_{ls}^2 are shown in red; those derived from χ_{jk}^2 are in green.

The minimization of the defined χ^2 is performed by using a Monte Carlo Markov Chain (MCMC) approach, running chains with 10^6 points and applying some priors on the parameters in the most general way possible, namely: $\bar{N} \geq 0$; $0 \leq b \leq 1$; $0 \leq \tilde{\epsilon} \leq 1$; $\tilde{L} > 0$; $f_1 > 0$, given that the GR limit is $f_1 \rightarrow 1$ and we need the first term in Eq. (5) to have attractive behaviour; and $\tilde{\delta}_1 > 0$. This last condition ensures that the $f(R)$ model we are considering works as a dark energy-type fluid, i.e. gives repulsive contribution to the gravitational potential. We could have considered also the case $\tilde{\delta}_1 < 0$, implying an attractive contribution to the gravitational potential and, thus, having the $f(R)$ theory mimicking a dark matter effect. However, such effect is quite controversial and questionable (see, for example, (Sotiriou & Faraoni 2010) and references therein), and would require a deeper theoretical study which is of course out of the purpose of this work. Thus, we stick to the only choice of a positive $\tilde{\delta}_1$.

Moving the discussion to the constraints we are able to put on the theoretical parameters, as it can be easily noted, in Table 1 we do not report results for the softening parameter $\tilde{\epsilon}$, which is definitely unconstrained, showing a basically uniform distribution all over the feasible range $[0, 1]$. On the other hand, as expected, \bar{N} is very well constrained in all cases, and there is no statistically significant difference between the values obtained with χ_{ls}^2 and χ_{jk}^2 . The clustering parameter b is mostly consistent with zero,

and only an upper limit can be set; this result indicates that the clusters in the catalog are not virialized (Yang & Saslaw 2012). Moreover, a similar trend has been noted also in literature, where smaller values of the cells correspond to smaller values of b (Sivakoff & Saslaw 2005; Rahmani et al. 2009; Yang & Saslaw 2012).

The interaction length \tilde{L} (which is a parameter characteristic of the gravitational theory considered), as well as b , is basically consistent with zero which is, incidentally, its GR limit. To be noted that \tilde{L} depends on f_1 and f_2 , which both enter the action of the $f(R)$ model and, thus, should be fixed by the theory to well determined values valid for all the gravitational structures once and for all. Instead, we have left them free to vary from one cluster to another in order to take into account possible local interactions leading the clusters far from the quasi-equilibrium condition. If we join the probability distributions from each and every cluster, we end up with a final joint estimation for the full sample, of $\tilde{L} = 0.47 \pm 0.09 Mpc$ for χ_{ls}^2 and of $\tilde{L} = 0.41 \pm 0.08 Mpc$ for χ_{jk}^2 . The two are very consistent with each other, but we cannot conclude that we do detect a deviation from GR, because we miss to check two other parameters, $\tilde{\delta}_1$ and f_1 .

And, in fact, the $f(R)$ -amplitude parameter $\tilde{\delta}_1$ itself is mostly consistent with zero, and only an upper limit can be set in most of the cases. In terms of the dimensional parameter δ_1 , assuming an average galaxy mass $10^{13} M_\odot$ (in (Ahmad et al. 2006) it has been shown that a mass range has secondary effects which are mostly negligible, so that to assume identical masses for galaxies, as it is usually done, is a good approximation), we easily find $\delta < \mathcal{O}(10^2)$. While it might seem a large signal, one must not forget it is coupled to an exponential term which drops fast its contribution. Moreover, while a time dependence is explicitly theoretically allowed for it, the data return no evidence for a possible evolution. Finally, the parameter f_1 is totally unconstrained. Note that for f_1 and for some cases of $\tilde{\delta}_1$ we have not given proper confidence intervals as best fit estimations, but we have only indicated some values in italic font, which correspond to the values assumed by the parameters exactly in the minimum of the two χ^2 previously defined. When this happens, it is because no statistics can be derived, due to a very noisy and irregular distribution. Note that for f_1 the values corresponding to the minimum in the χ^2 are somehow not physical (because of the degeneracies): very high values of f_1 would make the standard Newtonian part in the gravitational potential much smaller than what should be expected with respect to the new correction terms from the $f(R)$ gravity modifications.

Anyway, all this is not strange at all, due to very large degeneracies among all the parameters involved in the analysis. First of all, the quantity α_1 in Eq. (19) is strongly correlated with the value of f_1 , see Eq. (23); if $\tilde{\epsilon}$ is basically unconstrained, so it is α_1 and, as result, f_1 too. The impact of $\tilde{\epsilon}$ on α_2 , from Eq. (19), is smaller, but it is easy to see that $\alpha_2 \propto \tilde{\delta}_1 \tilde{L}$, so that we have another possible degeneracy between these two parameters. Anyway, as said, both $\tilde{\delta}_1$ and \tilde{L} (when single bin results are considered) are consistent with zero which is the limit for GR to apply, together with $f_1 \rightarrow 1$; but we are not in condition to check if it satisfied or not, due to the bad statistics related to this parameter.

As more general considerations, we can note how high

redshift clusters are fitted worse, in general, than smaller redshift ones; this could be due to the incomplete sampling from the catalog. The same reason might very likely be at the base of the trend in \bar{N} , which rises slightly with redshift, becomes practically constant, and then starts to decrease for $z > 0.45$. As we have explained above, the sample we are using is complete up to $z \sim 0.42$, after which we can have a bias toward smaller, namely, less massive, clusters (i.e. with smaller \bar{N}).

Finally, we also note that the larger is the cell volume (larger is R_1), the better is the fit. The bins $0.8 < R_1 < 0.9$ Mpc give unsatisfactory fits with both χ^2 definitions, at every redshift interval. In general, smaller redshifts have a better agreement, with $\chi_{i_s}^2$ fitting better small N values and around the peak in the distribution function; while $\chi_{j_k}^2$ gives better fit at high N . Cells slightly larger, with $0.9 < R_1 < 1.0$ Mpc, show a much better agreement between theory and data up to $z \sim 0.4$, with any difference between $\chi_{i_s}^2$ and $\chi_{j_k}^2$ barely distinguishable. At higher redshifts $0.4 < z < 0.55$, we fit data different, depending on the χ^2 , as described in the previous point; while data at very high redshifts $z > 0.55$ are not fit by the theoretical distribution. The largest cells, with $1.0 < R_1 < 1.1$ Mpc, instead, show remarkable agreement between theory and data, independently of the χ^2 definition used, up to $z \sim 0.55$, with slightly larger inconsistencies at higher redshifts, even if not so prominent as in previous cases.

8 DISCUSSION AND CONCLUSIONS

In this paper, we have studied the clustering of galaxies under the $f(R)$ gravity model. By assuming that the clustering of galaxies in an expanding universe evolves in a quasi-equilibrium manner through a sequence of equilibrium states, we have evaluated the gravitational partition function. With the help of resulting partition function, we have estimated the various equations of states of the such system where effects of $f(R)$ modifications are evident. In particular, we have derived explicit expressions for Helmholtz free energy, entropy, internal energy, pressure and chemical potential. The effects of $f(R)$ modifications on Helmholtz free energy and entropy are also analysed with the help of plot. We have found that modified gravity correction increases the value of the Helmholtz free energy. From the plot, we have seen that if modified gravity parameter $\delta_1(t)$ be increasing function of time, then the entropy is also increasing function of time, which is in agreement with the second law of the thermodynamics. Interestingly, we have found that the expressions of equations of states match with their standard expression except the form of clustering parameter which emerges naturally. The clustering parameter exhibits the effects of $f(R)$ modification. Since the system follows a quasi-equilibrium state, this enforces us to assume the system as a grand canonical ensemble. With this assumption, we have calculated the exact distribution function for the system which depends upon $f(R)$ corrected clustering parameter. We have discussed the critical temperature and conditions of stability also for the system. The resulting expression of specific heat obtained in case of $f(R)$ gravity justified the claim that at critical temperature the basic homogeneity of the system has been broken on the average inter-particle

scale by the formation of binary systems bounded gravitationally. We have obtained a relation between the clustering parameter and critical temperature, which estimates the critical value of clustering parameter at which the specific heat takes its maximum value. The effects of $f(R)$ modifications on the two-particle correlation function is also studied.

The feasibility of the gravitational quasi-equilibrium described in a thermodynamical way from the $f(R)$ -model has been also tested with observations. In particular we have made use of the distribution function of gravitational systems with extended mass interacting under $f(R)$ gravity given by Eq. (40), and describing how many galaxies are clustered/clustering in a spatial volume cell/region. We have used the cluster catalog described in (Wen & Han 2012), which provides the number of galaxies belonging to each of the $\sim 10^5$ clusters identified from the SDSS-III survey, together with their redshift and size. We have divided the full sample in spatial (by cluster's size) and time (by redshift) bins, under the condition they contain an enough large number of objects in order to have a good statistical description of the underlying distribution function, to verify the possibility of a space-time dependence of the same function. All these information make us able to try a fit of our theoretical results with real data. In order to perform the counts-in-cell analysis, we have divided the total sample in redshift bins with width $\Delta z = 0.05$, and radius bins with width $\Delta r_{200} = 0.1$ Mpc. From the obtained sub-groups, we have selected only those containing a sufficiently large number of clusters, ending with the groups corresponding to cell/cluster radii $0.8 < r_{200} < 0.9$, $0.9 < r_{200} < 1.0$ and $1.0 < r_{200} < 1.1$ Mpc, and to redshift $0.05 \leq z \leq 0.65$. By doing so, we must remember that the considered catalogue is complete up to a redshift $z \sim 0.42$, for clusters with an estimated mass $M_{200} > 1 \cdot 10^{14} M_\odot$; at higher redshift, a bias toward smaller clusters (lower masses) is possible (Wen & Han 2012).

On one hand, as shown in Figs. (5) - (6) - (7), the fit is quite remarkably good, except for a regime (high redshift tail and lower cluster size), for which a departure from the quasi-equilibrium description is visible. Very likely, this depends on the not-completeness of the used catalog in such regime; but also it is known from literature that the quasi-equilibrium is better verified (and more easily detectable) at scales much larger than the cluster's ones we are studying here. Anyway, as it is possible to see from Fig. (7), even for such strongly clustered systems, but with larger dimensions, we have a very good agreement between theory and observations.

On the other hand, we have too many free parameters entering in our analysis, and a lot of degeneracy among most of them, so that many have very poor constraints. This seems to be a problem of the $f(R)$ theory, more than the approach itself. In fact, the two parameters which are in common with GR, i.e. \bar{N} and b (the minimal number of parameters required to describe the clustering of galaxies in the thermodynamical quasi-equilibrium), are very well constrained and consistent with other results in literature. In particular, the very small values for b , which indicates a farer from equilibrium state of the cluster with the sizes we have considered. All the other parameters are more weakly constrained: the softening parameter $\tilde{\epsilon}$ (which is not a gravity theory parameter) is basically unconstrained; the dimension-

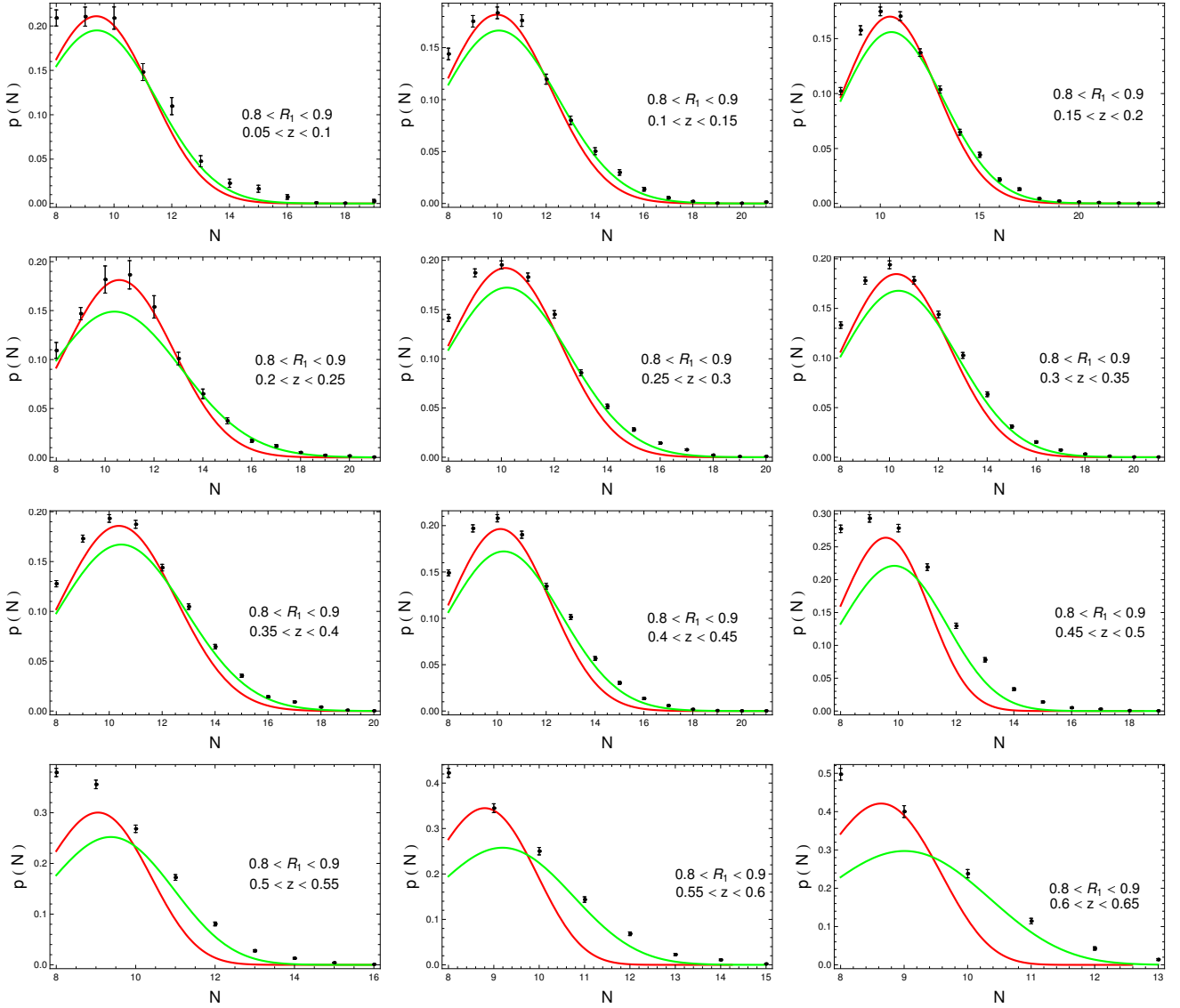


Figure 6. Comparison between data and theoretical expectation Eq. (40) for cell size bin $0.8 < R_1 < 0.9 \text{ Mpc}$. Black points: data; black bars: jackknife-like observational errors. Solid red line: best fit from minimization of χ^2_{ls} ; solid green line: best fit from minimization of χ^2_{jk} .

less interaction length of the $f(R)$ theory, \tilde{L} , is the best constrained parameter, but it is consistent with the GR value ($\tilde{L} \rightarrow 0$), and only an upper limit can be given for most of the clusters from the sample; the deviation from GR, $\tilde{\delta}_1$, is consistent with the GR limit, too, namely, ($\tilde{\delta}_1 \rightarrow 0$), but the related statistics is somehow invalidated by the last parameter, f_1 , which is always unconstrained and with very irregular confidence contours. In some way, f_1 is the elected capstone of all the degeneracies among all the parameters of our model.

In fact, we also have found that the fit is much better for the larger volume cells. The bins $0.8 < R_1 < 0.9 \text{ Mpc}$ give unsatisfactory fits with both χ^2 definitions, at every redshift interval. In general, smaller redshifts have a better agreement, with χ^2_{ls} fitting better small N values and around the peak in the distribution function; while χ^2_{jk} gives better fit at high N . Cells slightly larger, with $0.9 < R_1 < 1.0 \text{ Mpc}$,

show a much better agreement between theory and data up to $z \sim 0.4$, with any difference between χ^2_{ls} and χ^2_{jk} barely distinguishable. At higher redshifts $0.4 < z < 0.55$, depending on the χ^2 , data fits different; while data at very high redshifts $z > 0.55$ are not fit by the theoretical distribution. Interestingly, the largest cells, with $1.0 < R_1 < 1.1 \text{ Mpc}$, instead, show remarkable agreement between theory and data, independently of the χ^2 definition used, up to $z \sim 0.55$, with slightly larger inconsistencies at higher redshifts.

Thus, we conclude that the distribution function from the quasi-equilibrium approach might be used to constrain theories only if the number of additional parameters is small, and the correlation/degeneracy among them is strongly reduced. Then, we plan to use such approach with other than GR gravity models with such requirements.

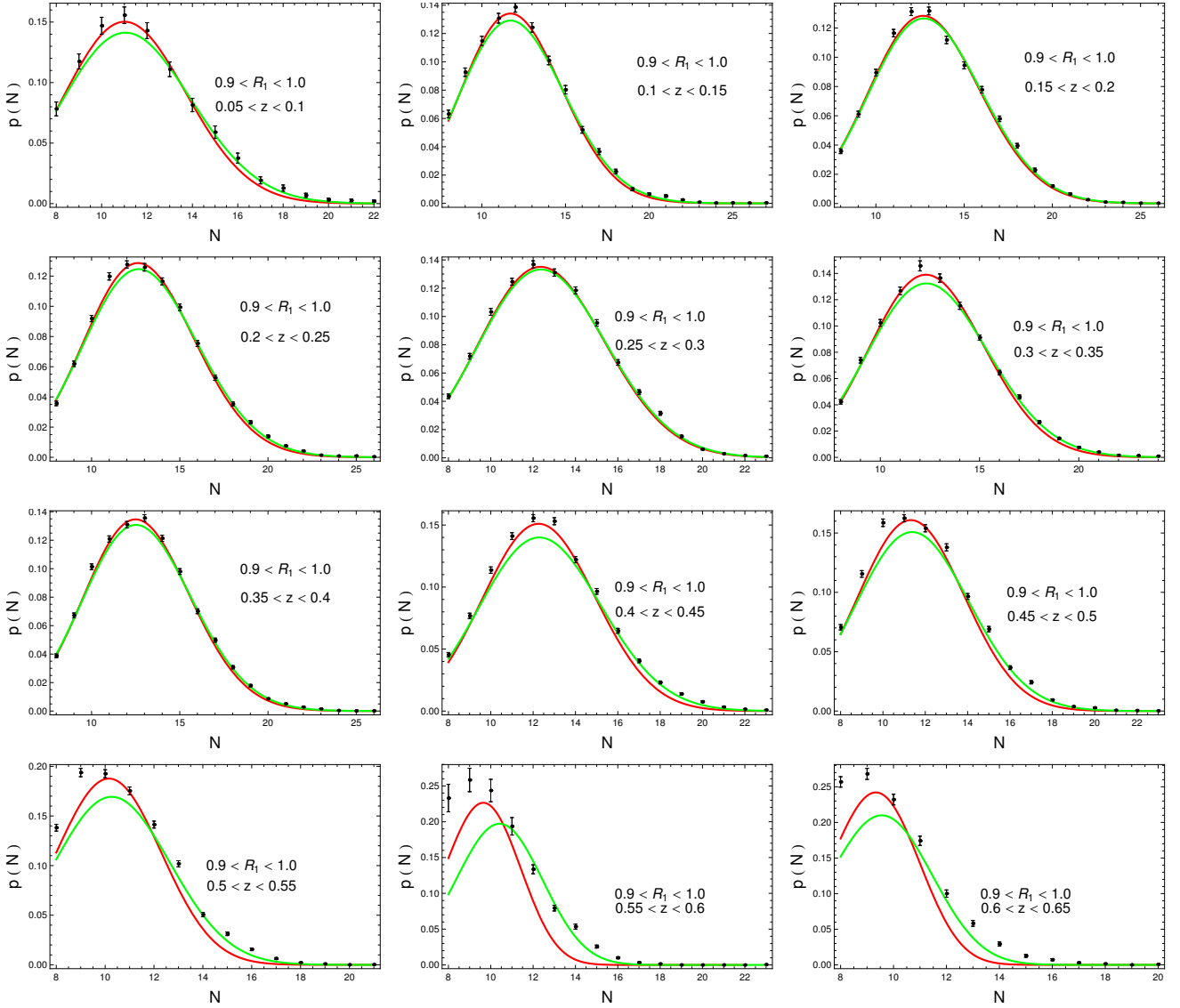


Figure 7. Comparison between data and theoretical expectation Eq. (40) for cell size bin $0.9 < R_1 < 1.0$ Mpc. Black points: data; black bars: jackknife-like observational errors. Solid red line: best fit from minimization of χ^2_{ls} ; solid green line: best fit from minimization of χ^2_{jk} .

ACKNOWLEDGEMENTS

V.S. is financed by the Polish National Science Center Grant DEC-2012/06/A/ST2/00395. Contribution from S.C. and V.S. is also based upon work from COST action CA15117 (CANTATA), supported by COST (European Cooperation in Science and Technology).

References

- Ahmad F., 1987, *Astrophys. Space Science* 129, 1
 Ahmad F., Saslaw W.C., Bhat N.I., 2002, *Astrophys. J.*, 571, 576
 Ahmad F., Saslaw W.C., Malik M.A., 2006, *Astrophys. J.*, 645, 940
 Capozziello S., Filippis E.D., Salzano V., 2009, *Mon. Not. Roy. Astron. Soc.*, 394, 947
 Capozziello S., De Laurentis, M., 2011, *Phys. Rept.*, 509, 167.
 Capozziello S., De Laurentis, M., 2012, *Annalen der Physik* 524, 545.
 Hameeda M., Upadhyay S., Faizal M., Farag Ali A., 2016, *Mon. Not. Roy. Astron. Soc.*, 463, 3699
 Hameeda M., Faizal M., Farag A. A., 2016b, *Gen. Relativ. Gravit.*, 48, 47
 Hills T. L, *Statistical Mechanics*, McGraw-Hill press, New York
 Hu B., Raveri M., Rizzato M., Silvestri A., 2016, *Mon. Not. Roy. Astron. Soc.*, 459, 3880-3889
 Hu W., Sawicki I., 2007, *Phys. Rev.*, D76, 064004
 Huang Q.-G., 2014, *JCAP* 02, 035
 Itoh M., Inagaki S., Saslaw W. C., 1993, *Astrophys. J.* 403, 476
 Kahya E.O., Khurshudyan M., Pourhassan B., Myrzakulov R., Pasqua A., 2015, *Eur. Phys. J. C* 75, 43
 Milgrom M., 1983 *Astroph. J.* 270, 365; 270, 371; 270, 384
 Nojiri S., Odintsov S.D. , 2011, *Phys. Rept.* 505, 59.
 Nojiri S., Odintsov S.D. , Oikonomou, V.K. 2017, *Phys. Rept.* 692, 1.
 Padilla N.D., et al., 2004, *Mon. Not. R. Astron. Soc.* 352, 211

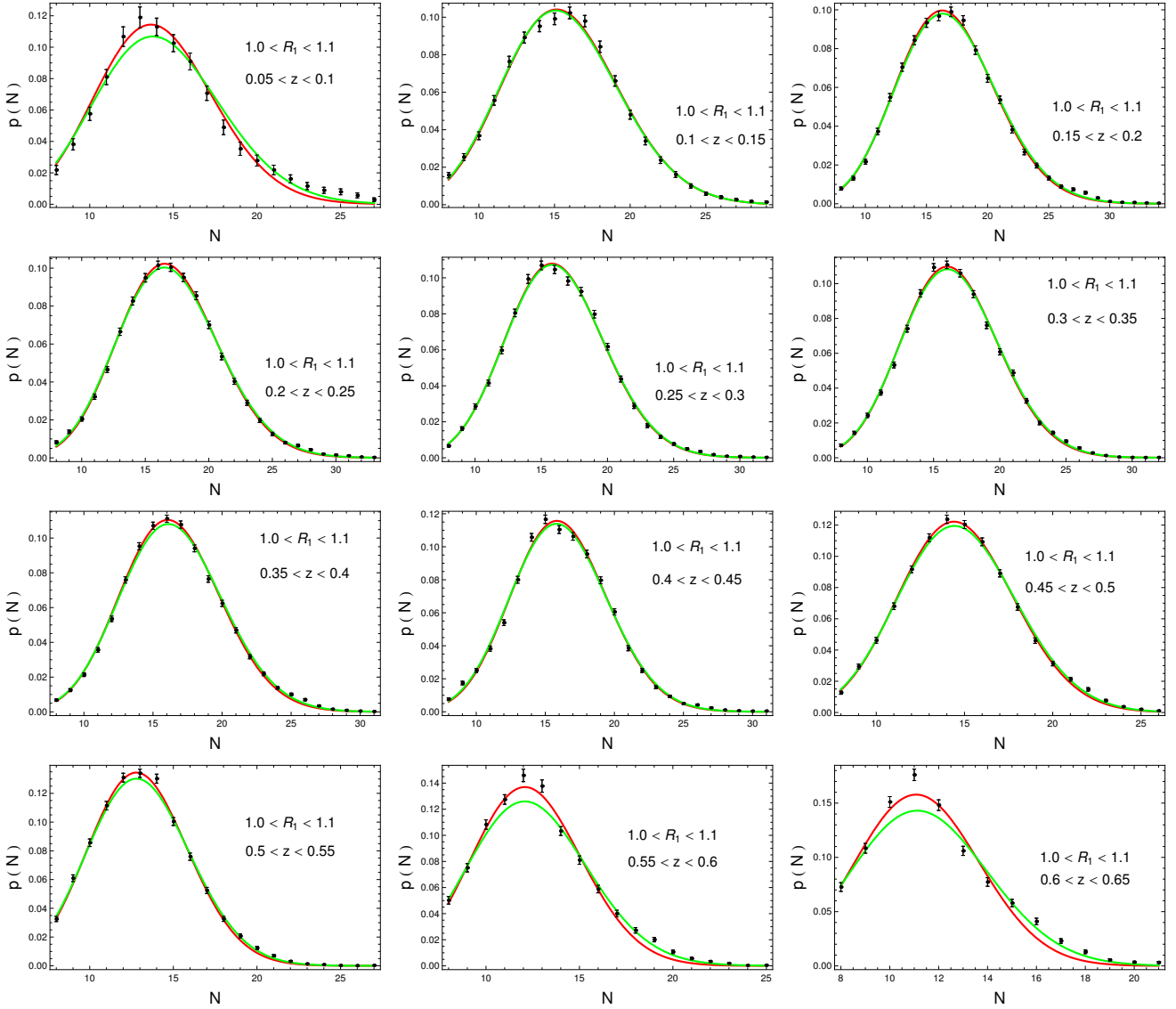


Figure 8. Comparison between data and theoretical expectation Eq. (40) for cell size bin $1.0 < R_1 < 1.1$ Mpc. Black points: data; black bars: jackknife-like observational errors. Solid red line: best fit from minimization of χ^2_{ls} ; solid green line: best fit from minimization of χ^2_{jk} .

Peebles P.J.E., 1980, *The Large Scale Structure of the Universe*, Princeton University Press, Princeton
 Pourhassan B., Upadhyay S., Hameeda M., Faizal M., 2017, *Mon. Not. Roy. Astron. Soc.*, 468, 3166
 Rahmani H., Saslaw W.C., Tavasoli S., 2009, *Astrophys. J.*, 695, 1121
 Sanders R., McGaugh S., 2002, *Ann. Rev. Astron. Astrophys.* 40, 263
 Saslaw W. C., 2000, *The distribution of the galaxies gravitational clustering in cosmology*, Cambridge University Press, Cambridge (2000)
 Saslaw W.C., Ahmad F., 2010, *Astrophys. J.*, 720, 1246
 Sadeghi J., Pourhassan B., Kubeka A.S., Rostami M., 2016, *Int. J. Mod. Phys. D* 25, 1650077
 Sotiriou T. P., Faraoni, V., 2010, *Rev. Mod. Phys.*, 82, 451-497
 Sivakoff G. R., Saslaw W. C., 2005, *Astrophys. J.*, 626, 795
 Upadhyay S., 2017, *Phys. Rev. D* 95, 043008
 Suto Y., Itoh M., Inagaki S., 1990, *ApJ*, 350, 492
 Wen Z. L., Han J. L., and Liu F. S., 2012, *Astrophys. J. Suppl.*,

199, 34
 Wen Z. L., Han J. L., 2015, *Astrophys. J.*, 807, 2
 Yang A., Saslaw W.C., 2011, *Astrophys. J.*, 729, 123
 Yang A., Saslaw W.C., 2012, *Astrophys. J.*, 753, 113

This paper has been typeset from a $\text{\TeX}/\text{\LaTeX}$ file prepared by the author.